Evolution of Nitrogen Oxide Chemistry in the Nocturnal Boundary Layer

S. GALMARINI* AND P. G. DUYNKERKE

IMAU, Utrecht University, Utrecht, the Netherlands

J. VILÀ-GUERAU DE ARELLANO

Departamento de Fisica Aplicada, Universidad Politecnica de Catalunia, Barcelona, Spain

(Manuscript received 15 August 1996, in final form 23 October 1996)

ABSTRACT

The nocturnal cycle of nitrogen oxides in the atmospheric boundary layer is studied by means of a one-dimensional model. The model solves the conservation equations of momentum, entropy, total water content, and of five chemical species. The chemical cycle relates to the nighttime conversion of NO, NO_2, and O_3 into HNO_3 via NO_3 and N_2O_5. For simplicity, only homogeneous chemical reactions are considered. The turbulent fluxes of momentum, temperature, and moisture and of the chemical species are determined by means of a second-order closure model. The fluxes of the chemically reactive species are determined by explicitly taking into account the chemical transformation during the transport process. The one-dimensional model simulates a stable boundary layer with typical rural concentrations of the above-mentioned species. To study the effect of heterogeneous mixing due to the strong gradients of temperature and concentrations, the authors compare the one-dimensional model results with the results obtained with a box model. The study demonstrates that the concentration of NO plays a considerable role in the formation of NO_3, N_2O_5, and HNO_3. The reduced activity of turbulent transport shows that the chemical activity in the boundary layer can be decoupled from that of the so-called reservoir layer. The stability conditions induce inhomogeneous distribution of the species in the vertical direction and the formation of large concentration gradients. In these conditions, the study of the process by means of a box model can lead to an inaccurate estimate of the concentrations of species like NO and NO_3.

1. Introduction

The nocturnal boundary layer (NBL) is an important stage in the 24-h evolution of the atmospheric boundary layer. During the night, the diurnal convective conditions are suppressed by the cooling of the surface, which generates stable stratification. In a stably stratified layer a trace gas may accumulate close to the surface. In fact, under these conditions the turbulent transport produced by the wind shear is reduced by the negative buoyancy (Rao and Snodgrass 1979).

In the NBL nitrogen oxides follow different pathways from the ones they follow during daytime hours in the convective boundary layer (CBL) (Seinfeld 1986; Finlayson-Pitts and Pitts 1986; Warnek 1988). The absence of solar radiation during the night reduces the number of chemical reactions, but chemical species that are not important in the daytime CBL can play an important role during the night in the NBL. The nighttime chemical processes generally lead to the formation of either reservoir species (i.e., species that will be reconverted into their precursors during daytime) or to the formation of species that will be removed by deposition processes. The turbulent transport and the chemical transformation during nighttime conditions need to be described accurately if the concentrations on the following day are to be predicted correctly.

When modeling the turbulent transport of chemically reactive species in the atmospheric boundary layer one has to take into account the combined processes of turbulent transport and chemical transformation. Recent studies have analyzed the problem of turbulent transport of chemical compounds in the surface layer (e.g., Fitzjarrald and Lenschow 1983; Galmarini et al. 1997b), in the neutral boundary layer (e.g., Gao and Wesley 1994), and in the convective boundary layer (e.g., Schumann 1989; Sykes et al. 1994). All these works have emphasized the importance of treating the turbulent transport and chemical reaction process simultaneously to obtain a correct estimate of the mass transported by the turbulent flow and of the rates of transformation. Because turbulent transport and chemical transformation constitute a combined process, the turbulent flux of a chemically reactive species, which is represented by the correlation between velocity fluctuations and concentration

*Current affiliation: JRC ISPRA, Ispra, Italy.

Corresponding author address: Stefano Galmarini, JRC ISPRA, TP321, 21020 Ispra (Va), Italy.
E-mail: stefano.galmarin@jrc.it

fluctuations, it varies due to the effect of the chemical transformation on the fluctuations. For a correct estimate of the quantity of mass transported by the turbulent flow it is therefore necessary to take into account the chemical transformation as production/depletion of the flux. Furthermore, the fact that turbulence is the process that governs the mixing of reactants and consequently their molecular contact and chemical reaction implies that the efficiency of the turbulent mixing governs the efficiency of the chemical reaction (Donaldson and Hilst 1972). The state of mixing of the species, which is represented by the covariance of the reactant concentration fluctuations, should in principle be taken into account in models of the turbulent transport of chemically reactive species. Past studies have also emphasized that turbulent transport and chemical processes have to be considered simultaneously if the species concerned have a chemical lifetime that is comparable to the lifetime of the turbulent transport. Among the species with these characteristics are the nitrogen oxides. The latter, furthermore, constitute a very important group of compounds in nighttime chemistry.

When chemical reactions occur in a stably stratified boundary layer an additional factor needs to be considered. The presence of a stable stratification gives rise to inhomogeneous vertical distribution of the tracer (e.g., Neu et al. 1994). Under very stable conditions a tracer released at the surface may be confined to the stable boundary layer and a tracer present above the boundary layer may be slowly entrained and transported downward by the reduced turbulent transport. When the time evolution of the concentration of the species is determined by means of models that have a coarse spatial resolution (like the majority of large-scale atmospheric chemistry models), errors may arise due to the fact that the inhomogeneous vertical distribution of the species is only roughly resolved. In the case of chemically reactive species, this can have important consequences for their rate of production/depletion (Vilà-Guerau de Arellano et al. 1993; Pyle and Zavody 1990; Chatfield et al. 1990).

The main purpose of this study is to analyze in detail the behavior of chemically reactive species in the NBL. The chemical species considered are nitrogen oxides. Because the study concentrates on nocturnal conditions a specific chemical scheme has been selected. This scheme involves NO_3, N_2O_5, and HNO_3 as well as the daytime triad NO, NO_2, O_3. This chemical scheme has been chosen because it is essential and representative for the nocturnal chemistry (Warneck 1988). By means of a one-dimensional model we describe the formation and time evolution of the NBL together with the turbulent transport and the chemical transformation of the species. The effect of chemical transformation on the flux of the species and the effect of the state of mixing of the species on the efficiency of the chemical reaction are explicitly taken into account by means of a second-order closure model. The approach we used is based on an extension of surface-layer similarity theory to chemically reactive species (Vilà-Guerau de Arellano et al. 1995) and on the fact that the similarity theory is locally applicable to the stable boundary (Nieuwstadt 1984).

The detailed one-dimensional model simulation is compared with the simulation obtained with a box model in order to determine the applicability of this simpler approach to the description of the nighttime chemistry of nitrogen oxides and to determine the effect of heterogeneous vertical distribution of the stable boundary layer on the chemical transformation.

2. Model description

a. Governing equations

The nocturnal-chemistry model solves the one-dimensional conservation equations of momentum [(1) and (2)], entropy (3), total water content mixing ratio (4), and of six chemical species [(5), see section 2b for the specific chemical scheme]:

$$\frac{\partial U}{\partial t} = f(V - V_g) - \frac{\partial \overline{uw}}{\partial z} \tag{1}$$

$$\frac{\partial V}{\partial t} = -f(U - U_g) - \frac{\partial \overline{vw}}{\partial z} \tag{2}$$

$$\frac{\partial \Theta}{\partial t} = -\frac{\partial \overline{w\theta}}{\partial z} \tag{3}$$

$$\frac{\partial Q}{\partial t} = -\frac{\partial \overline{wq}}{\partial z} \tag{4}$$

$$\frac{\partial C_i}{\partial t} = -\frac{\partial \overline{wc_i}}{\partial z} + \text{sign} \sum_{\substack{j,m \\ m \le j}}^{M} k_{mj}(C_m C_j + \overline{c_m c_j}) + \text{sign} \sum_{j}^{N} k_j C_j. \tag{5}$$

As a result of the application of the Reynolds decomposition, the instantaneous variables are given by a mean (uppercase letters) and a turbulent (lowercase letters) component. Overbars represent ensemble means. Equations (1)–(5) are obtained by assuming a horizontally homogeneous atmosphere. In (1), U_g and V_g are the two components of the geostrophic wind and f the Coriolis parameter. The terms $\overline{uw}$ and $\overline{vw}$ in (1) and (2), respectively, are the two components of the Reynolds stress; $\overline{w\theta}$, $\overline{wq}$, $\overline{wc_i}$ are the turbulent fluxes of the considered scalars. In Eq. (5) we find from left to right the time evolution of the mean concentration, the vertical divergence of the turbulent flux, and two chemistry terms. These are expressed in a general formulation where M and N are the total numbers of second- and first-order chemical reactions, respectively, which involve C_i as a reactant (sign = −1) or a product (sign = 1). The terms k_{mj} and k_j are the rates of the chemical reactions. In expression (5), $\overline{c_m' c_j'}$ is the concentration covariance that

arises from Reynolds averaging of the concentration product that appears in the chemical term. In physical terms, $\overline{c_m' c_j'}$ represents the state of mixing of the species, and within the first term of expression (5) it gives the influence of inhomogeneous turbulent mixing on the second-order chemical transformation (Donaldson and Hilst 1972). Examples of the application of the dynamical and theromodynamical part of the model can be found in Duynkerke (1991) where the model was used to study the formation of radiative fog and in Galmarini et al. (1997a) where the time evolution of the NBL was compared with large-eddy simulation results. In this study we will mainly show the results relating to the inert scalars and to the chemically reactive species.

Before solving Eq. (5), we have to determine the turbulent flux of concentration ($\overline{wc_i}$) and the concentration covariance that appears in the chemical term. The turbulent flux $\overline{wc_i}$ is closed according to

$$\overline{wc_i} = -K_{C_i} \frac{\partial C_i}{\partial z}, \tag{6}$$

where K_{C_i} is the eddy exchange coefficient of the species C_i. Here, the turbulent flux has been expressed as a function of the concentration gradient rather than the gradient of the mixing ratio since the analysis will be limited to a shallow portion of the boundary layer (Venkatram 1993; Webb et al. 1980). The explicit formulation of the eddy exchange coefficient is given by

$$K_{C_i} = \frac{(\kappa z)^2}{\Phi_{C_i} \Phi_m} \left| \frac{\partial \mathbf{M}}{\partial z} \right|, \tag{7}$$

where κ is the von Kármán constant (equal to 0.4), z the distance from the surface, **M** the mean wind vector, and Φ_m and Φ_{C_i} are the flux-gradient relationships of momentum and of the species, respectively. The terms Φ_m and Φ_{C_i} determine the dependence of the eddy-exchange coefficient on the atmospheric local stability (Nieuwstadt 1984; Sorbjan 1986a). If the species are inert, Φ_{C_i} is the flux-gradient relationship of heat (Φ_h). In the case of chemically reactive species, Φ_{C_i} is not only a function of the stability as in the case of an inert tracer but it also depends on chemistry-dependent parameters like the ratio of the timescale of turbulence to the timescale of the chemical processes that C_i undergoes (Damköhler number) and the ratio of the local fluxes of the chemical species involved with C_i in the chemical transformation. The flux-gradient relationships appearing in (7) are calculated by means of a second-order closure model (Vilà-Guerau de Arellano et al. 1995). This approach allows one to consider the chemical transformation as a production/depletion term of the flux of the chemical species. The second-order closure model has been developed on the basis of surface-layer similarity theory and is applicable to any stability condition. In this study, the similarity theory for chemically reactive species is extended to the NBL according to the local-similarity theory proposed by Nieuwstadt (1984). The concentration covariance appearing in Eq. (5) is also obtained from the second-order closure model by the explicit solution of its conservation equation where the chemical terms have been explicitly taken into account. The complete closure-model formulation can be found in Galmarini et al. (1997b).

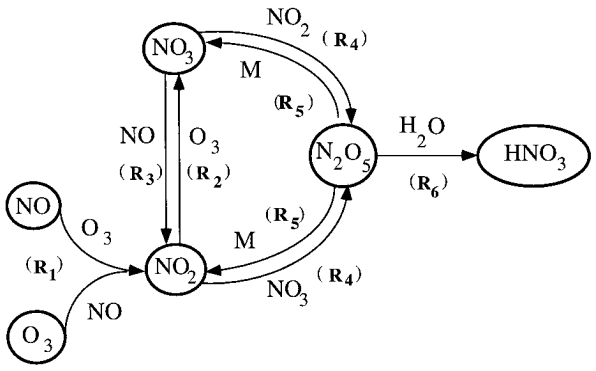

FIG. 1. The nocturnal chemistry scheme. In the figure, "M" denotes a neutral molecule acting as an energy-transferring body.

b. The chemical scheme

The chemical scheme considered is the inhomogeneous nighttime chemical scheme of nitrogen oxides. For simplicity, only gas phase transformations have been taken into account. The scheme considers the following chemical reactions:

$$\mathrm{NO} + \mathrm{O_3} \xrightarrow{k_1} \mathrm{NO_2} + \mathrm{O_2} \tag{R1}$$

$$\mathrm{NO_2} + \mathrm{O_3} \xrightarrow{k_2} \mathrm{NO_3} + \mathrm{O_2} \tag{R2}$$

$$\mathrm{NO} + \mathrm{NO_3} \xrightarrow{k_3} 2\ \mathrm{NO_2} \tag{R3}$$

$$\mathrm{NO_2} + \mathrm{NO_3} \xrightarrow{k_4} \mathrm{N_2O_5} \tag{R4}$$

$$\mathrm{N_2O_5} + \mathrm{M} \xrightarrow{k_5} \mathrm{NO_3} + \mathrm{NO_2} \tag{R5}$$

$$\mathrm{N_2O_5} + \mathrm{H_2O} \xrightarrow{k_6} 2\ \mathrm{HNO_3}. \tag{R6}$$

Reactions (R1)–(R6) account for the conversion of the daytime triad NO–NO_2–O_3 into HNO_3 (nitric acid). This process takes place via NO_3 (nitrate radical) and N_2O_5 (dinitrogen pentoxide) as indicated in Fig. 1. NO_3 and N_2O_5 can generally be considered as reservoirs of NO, NO_2, and O_3 during the nighttime period (Solomon et al. 1989; Wayne et al. 1991), whereas HNO_3 serves as a removal species since it is deposited on the surface and removed by heterogeneous processes. From Fig. 1 we can see that the system is generally tending toward NO_2, which becomes the first reservoir of NO and O_3. These species are simply removed from the chemical system, and NO_2 production also depends on the back-

ward transformation of N_2O_5 [reaction (R5)]. The final removal of NO_2 from the system takes place via the reaction of N_2O_5 with water vapor that produces HNO_3. Other nitrogen oxides like N_2O_3 and N_2O_4, present during nighttime conditions, may be neglected because they are present in only negligible concentrations (Warnek 1988). NO_3 and N_2O_5 represent very important species in atmospheric chemistry. In general they are responsible for the removal of NO_2 and they determine the oxidation capacity of the atmosphere during nighttime and its acidification via the formation of HNO_3 (Wayne et al. 1991). Important also is the heterogeneous chemistry of NO_3 and N_2O_5 (Dentener and Crutzen 1993), which is not considered in this study. The reaction rates of the chemical scheme (R1)–(R6) are given in Atkinson et al. (1992) and are presented in the appendix. Although Atkinson mentioned that reaction (R6) may be driven by heterogeneous processes only, we assume that N_2O_5 reacts homogeneously with water vapor at reaction rate k_6.

Past studies (Johnston et al. 1986; Davidson et al. 1990) have indicated the possible presence, in nighttime conditions, of other reactions that produce NO and O_2 from NO_3. Furthermore, England and Corcoran (1974) suggest the presence of an extra NO_2 loss mechanism via the reaction with H_2O. However, Russell et al. (1986) and recent smoke-chamber experiments (Mentel and Wahner 1997) dispute the relevance of these reactions. There are still uncertainties about the reaction rates, and investigations are continuing. Many questions remain about the chemical behavior of nighttime species and especially of NO_3 and N_2O_5 (Wayne et al. 1991). These relate to the reactions of NO_3 with organic nonradical species like alkenes, phenolic, and heterocyclic compounds; sulphur compounds and radicals; as well as the heterogeneous chemistry mechanisms (Mozurkewich and Calvert 1988). Nevertheless, the chemical cycle (R1)–(R6) represents a complete scheme for the gas-phase nocturnal chemistry of nitrogen oxides and is an appropriate system by which to investigate the combined processes of turbulent transport and chemical reaction. In fact, reactions (R1)–(R6) can generally be considered to be very fast (Galmarini et al. 1995; Ljungström and Hallquist 1996) and to have timescales comparable with the timescale of turbulent transport. Under these circumstances, therefore, it is necessary to consider the effect of the chemical transformation on the reaction of the species and the dependence of the chemistry efficiency on the mixing capacity of turbulence.

The reaction rates of (R1)–(R5) are temperature dependent (see appendix). This dependence has been explicitly taken into account in the model simulation. The reaction rates are thus time- and space-dependent quantities due to the time evolution and the vertical profile of the temperature in the NBL.

3. Model results

a. Boundary and initial conditions

We simulated a typical NBL at 45° latitude driven by a geostrophic wind of 10 m s^{-1} in the zonal direction and zero in the meridional direction. We assumed constant surface cooling of 10 W m^{-2} (8×10^{-3} K m s^{-1}). The surface roughness for momentum and heat are 0.1 m and 0.1×10^{-5} m, respectively. The radiative flux divergence in the mean potential temperature equation was not taken into account because of the wind speed chosen (Estournel and Guedalia 1985).

The specific humidity at the surface is 6×10^{-3} kg kg^{-1} and decreases linearly with height (expressed in meters) according to

$$q\,(z, 0) = 5.9 \times 10^{-3} - 0.1 \times 10^{-6} z \text{ (kg kg}^{-1}\text{)}.$$

The temperature initial profile is given by

$$T\,(z, 0) = 11 - 1 \times 10^{-2} z \text{ (°C)},$$

where the lapse rate is assumed to be adiabatic. For the initial conditions considered, the boundary layer shows no substantial formation of liquid water during the simulated period of time; therefore, the total water can be considered to be in the gas phase.

The initial conditions for the chemical species are those that can be expected in the boundary layer at the end of the day in a rural area. Here, O_3 is assumed to be well mixed in the boundary layer and to have a constant concentration of 25 ppb. NO and NO_2 are also assumed to be well mixed and to have a concentration of 0.25 ppb and 4 ppb, respectively. NO is kept constant at the surface to ensure a continuous emission, whereas, for the purpose of calculating the fluxes near the surface, we assume that NO_2 and O_3 are zero at the surface. NO is assumed to have zero concentration at the upper boundary. The NO emission resulting from the fixed surface concentration is 0.006 ppb m s^{-1}; this value has been averaged over the simulated time (see next section). Concentrations of O_3 similar to those used as initial conditions for the case study were measured in a rural area by Harrison et al. (1978).

The other nitrogen oxides NO_3, N_2O_5, and HNO_3 are assumed to be zero everywhere in the domain at the beginning of the simulation and zero at the surface throughout the simulation period. The zero concentration assumption for NO_3 and N_2O_5 is based on the measurements obtained by Platt et al. (1980, 1981, 1984) and Pitts et al. (1984). This assumption allows us to make a more detailed study of the behavior of these species as reservoirs for NO, NO_2, and O_3 during the night in a stable boundary layer. During the day, NO_3 is photolysed very rapidly and its concentrations are below the present instrument detection limits (less than 1 part per trillion) (Mihelcic et al. 1993). HNO_3 does not give feedback to the system since it is only produced and deposited; for this species, therefore, the zero concentration assumption as initial condition does not in-

TABLE 1. Scaling parameters of the NBL simulation.

u_* (m s^{-1})	θ (K)	q_* (g kg^{-1})	h (m)	L (m)
0.28	0.036	0.1	225	176.5

fluence the results. At the surface, all the chemical species are assumed to encounter resistance. The values of the resistances for each species have been derived on the basis of the deposition velocities calculated by Gao and Wesely (1994).

The conservation equations of momentum, entropy, and of the seven species are integrated over a period of 12 h and a domain of 500 m on a 41-level logarithmically spaced staggered grid. The averaging time is based on the 5-min output and the variables are scaled before time averaging.

b. Stable boundary layer characteristics

The NBL that develops from the above-mentioned boundary and initial conditions is characterized by the following scaling quantities. In Table 1, u_* is the friction velocity, θ_* the temperature scale, and q_* moisture scale. These are defined, according to surface-layer similarity theory, as

$$u_* = (\overline{uw}_0^2 + \overline{vw}_0^2)^{0.25}; \quad \theta_* = -\frac{\overline{w\theta}_0}{u_*}; \quad q_* = -\frac{\overline{wq}_0}{u_*},$$

where the subscript 0 denotes the surface value. The height of the boundary layer h is the height where the turbulent flux of temperature is 5% of the surface value (Mahrt and Heald 1979). From the values of h and the Monin–Obukhov length scale L, one can see that the boundary layer is stable. The values summarized in Table 1 have been averaged over the whole simulation period. The stable boundary layer approaches a quasi-steady-state condition approximately 2 or 3 h after the beginning of the simulation, as indicated by the linear temperature flux profile. Despite the time required to reach steady state, in the results presented farther on we have disregarded only the first hour of the simulation in order to guarantee a more complete description of the time evolution of the chemical species.

c. Time and space evolution of the mean concentrations of the chemical species

Figures 2a–f show the time series of the concentration vertical profiles of the six chemical species of the scheme (R1)–(R6). The concentrations are plotted as a function of z/h to emphasize the differences between the mean concentration in the boundary layer and the mean concentration in the reservoir layer. The latter usually identifies the layer above the NBL (Stull 1988). The color palette shows the minimum and the maximum concentrations (ppb) of each of the species. The main features of the concentration distribution can be summarized as follows.

- NO (Fig. 2a): The concentration of NO decreases rapidly with height due to the reaction with O_3. Here, NO does not extend beyond 10% of the boundary layer depth. About 4 h after the beginning of the simulation, NO starts to accumulate close to the surface due to the presence of the emission flux at the surface.
- O_3 (Fig. 2b): In the reservoir layer ($z/h > 1$), the ozone concentration is fairly constant. At this height, the only sink for ozone is the reaction with NO_2 (R2). Within the boundary layer the concentration of ozone constantly decreases with time due to the presence of NO_2 throughout the boundary layer and the presence of NO close to the surface. A neat separation between the concentration in the boundary layer and in the reservoir layer appears around the sixth hour of the simulation.
- NO_2 (Fig. 2c): A rapid and constant decrease in NO_2 is shown in the reservoir layer and in the boundary layer. In the boundary layer, a concentration maximum develops at around 10% of the boundary layer height. The maximum can be attributed to the presence of NO and O_3, which produce NO_2 (R1). The absence of NO in the reservoir layer and the activity of the chemical sinks in NO_2 [reactions (R2) and (R4)] cause a constant decrease of NO_2 concentration with time. The development of a maximum concentration again emphasizes the different behavior of the boundary layer chemistry and the reservoir-layer chemistry. The decrease in NO_2 with time is consistent with the chemical scheme considered (Wayne et al. 1991).
- NO_3 and N_2O_5 (Figs. 2d and 2e): The different behavior of the boundary layer concentration and the reservoir layer concentration is also clear for NO_3. NO_3 shows a maximum concentration constant in time in the reservoir layer and a constant decrease in both space and time within the NBL. In the reservoir layer the abundance of O_3 and the presence of NO_2 constantly produce NO_3, whereas in the boundary layer the reduced O_3 concentration, the reaction of NO_3 with NO_2 (R4), and that of NO_3 with NO (R3) close to the surface cause a decrease in the NO_3 concentration with time. In the middle of the boundary layer a maximum concentration forms within the first 2 h and a constant decrease is observed with time. This characteristic feature was observed by Platt et al. (1980) during the Riverside campaign. The results of Fig. 2 agree with the measurements made by Platt et al. (1980) also with regard to the correlation they found between NO_3 with O_3 in both time and space.

  N_2O_5 shows a maximum of concentration a few hours after the beginning of the night and a gradual decrease as the night proceeds due to its conversion into HNO_3.
- HNO_3 (Fig. 2f): The largest concentration of HNO_3 is found between 8 and 11 h in the reservoir layer. In

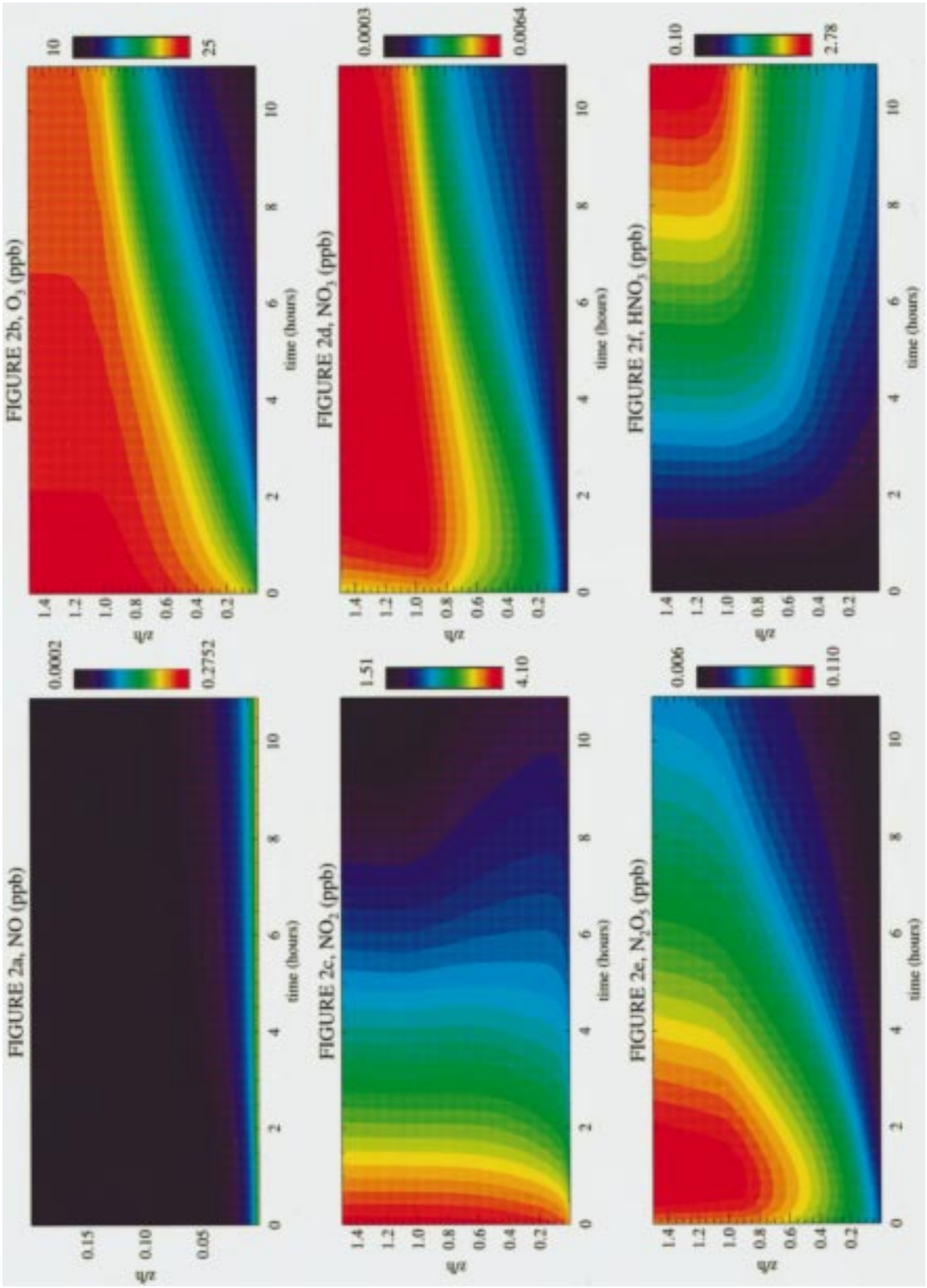

FIG. 2. (a)–(f) Time evolution of the vertical profile of the six chemical species of the scheme (R1)–(R6). The contours are expressed as a function of dimensionless height z/h (the time averaged value of h is equal to 225 m). The color palette indicates the minimum and maximum concentrations (ppb) for each of the species: (a) NO, (b) O_3, (c) NO_2, (d) NO_3, (e) N_2O_5, and (f) HNO_3.

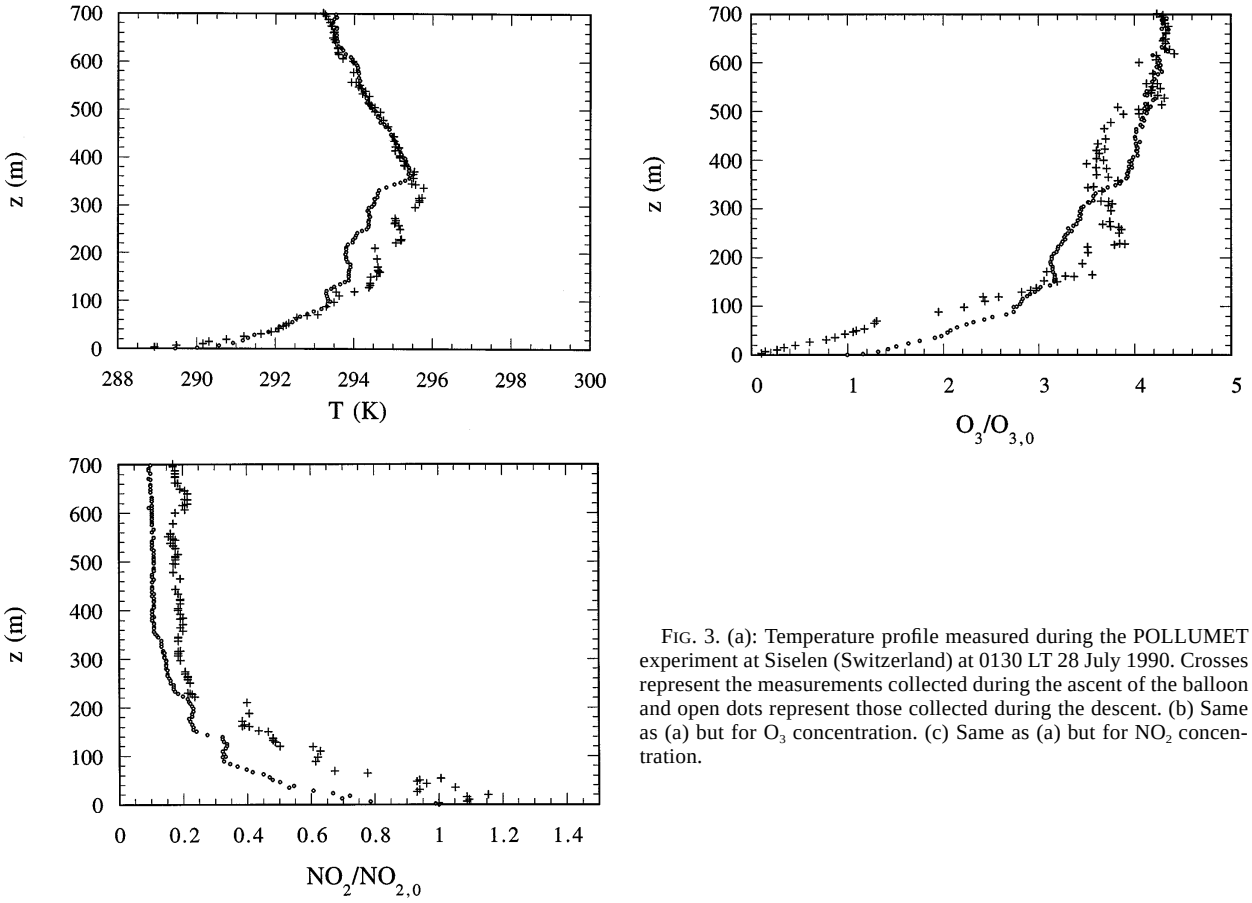

FIG. 3. (a): Temperature profile measured during the POLLUMET experiment at Siselen (Switzerland) at 0130 LT 28 July 1990. Crosses represent the measurements collected during the ascent of the balloon and open dots represent those collected during the descent. (b) Same as (a) but for O_3 concentration. (c) Same as (a) but for NO_2 concentration.

the boundary layer the concentration decreases rapidly toward the surface due to the reduced chemical production of N_2O_5 and the strong HNO_3 deposition process at the surface. Aircraft measurements made by LeBel et al. (1990) indicate larger concentrations of HNO_3 in the boundary layer than in the troposphere in nighttime conditions. The measurements also point to large space variability and sensitivity of the measurements to the presence of anthropogenic local sources. Just like NO_3, N_2O_5 rapidly increases in the first 2 h reaching a clear concentration maximum. By the end of the simulation period HNO_3 anticorrelates with NO_2.

The results show that the chemistry of the NBL tends to be decoupled from that of the reservoir layer. This decoupling leads to different distributions of the species. The process is caused by the formation of the NBL and the negligible exchanges of mass between the NBL and the reservoir layer (see next section). It also appears that the limited vertical distribution of NO plays an important role in the evolution of the other species. Results similar to those presented above were obtained during the Air Pollution and Meteorology (POLLUMET) experiment, as can be seen from Figs. 3a–c. The O_3 and NO_2 concentrations were measured during the campaign of Siselen (Switzerland) on the night of 28 July 1990 at 0130 local time by means of sondes attached to a balloon. In Figures 3b and 3c the concentration profiles have been normalized with the surface values (12.5 ppb and 20.2 ppb for NO_2 and O_3, respectively). For details about the experimental campaign, the site, and the instrumentation, see Neu et al. (1994) and Wanner et al. (1993). The temperature profile (Fig. 3a) clearly shows the presence of a boundary layer with a temperature inversion at 300 m. The concentration of O_3 and NO_2 also show two distinct profiles within the boundary layer and the reservoir layer.

d. Turbulent fluxes and concentration covariances

Figures 4a–f show the 11-h-averaged flux profiles for the six chemical species. The fluxes of the species are normalized with $u_* c_{iM}$, where c_{iM} is defined as

$$c_{iM} = -\frac{\max(|\overline{wc_i}|)}{u_*}$$

and represents the maximum concentration scale.

Table 2 gives the 11-h-averaged values of the scaling parameters for the chemical species of the scheme (R1)–(R6). The order of magnitude of the fluxes found is in

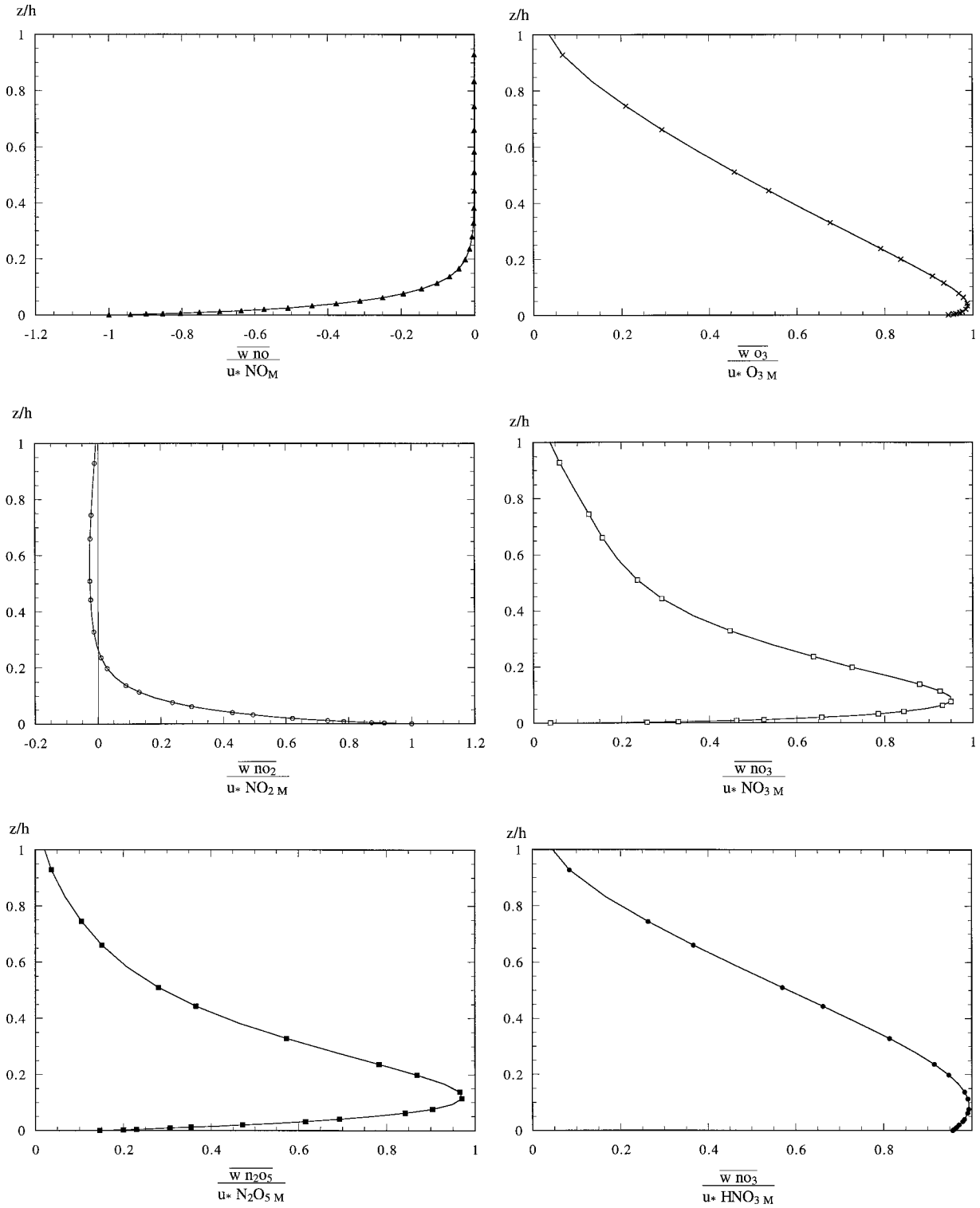

FIG. 4. (a)–(f) Nondimensional flux profiles of the chemical species of the scheme (R1)–(R6). Each species flux is normalized with the maximum flux value: (a) NO, (b) O_3, (c) NO_2, (d) NO_3, (e) N_2O_5, and (f) HNO_3.

TABLE 2. The time-averaged scaling parameters for the flux profiles of the six chemical species.

NO_M (ppb)	O_{3M} (ppb)	NO_{2M} (ppb)	NO_{3M} (ppb)	N_2O_{5M} (ppb)	HNO_{3M} (ppb)
−0.022	0.043	0.008	2.29×10^{-5}	3.34×10^{-4}	2.9×10^{-3}

agreement (at least as far as NO and O_3 are concerned) with surface measurements made by Wesley et al. (1989) and by Slemr and Seiler (1984) during nighttime hours. As can be seen from Fig. 4, as a consequence of the chemical activity (Fitzjarrald and Lenschow 1983) no species shows the linear profile expected for a scalar in conditions of steady state and horizontal homogeneity (Nieuwstadt 1984). All the species have negative fluxes throughout the NBL, the only exception being NO and NO_2 above $0.2z/h$. As in the case of the mean concentration, the flux of NO does not extend further than $0.2z/h$. The change of sign of the flux of NO_2 is due to the local production of mean concentration, which generates a positive vertical flux.

The flux profiles of O_3, NO_3, N_2O_5, and HNO_3 show that maximum values are found close to the surface ($0.1z/h$). The maximum O_3 flux can be attributed to the limited extension of NO in the vertical. The maximum in fact occurs at $0.5z/h$ where the NO starts to vanish. From this position downward toward the surface, the concentration of O_3 undergoes maximum depletion due to NO and NO_2 and thus generates the largest concentration gradients. The values of the entrainment fluxes of the six chemical species are given in Table 3. The prevailing entrainment fluxes are those of O_3 and HNO_3. This is consistent with the mean concentration profiles where a clear concentration jump is shown across the height of the boundary layer.

As mentioned earlier, in order to determine the turbulent fluxes of the species we used the second-order closure model that accounts for the correction due to the chemical transformations. In this way, we are able to determine the influence of chemistry on the flux of the species under conditions of stable stratification. For the chemical scheme considered, the chemistry has been accounted for in the second-moment conservation equations of all the species considered, the only exception being HNO_3. For the neutral boundary layer, Gao and Wesely (1994) determined the insensitivity of this species flux to chemical transformation but underlined the implications of the chemical transformation for species like NO_2, NO_3, and N_2O_5. Figure 5 shows the flux-gradient relationship of NO, O_3, NO_2, N_2O_5, and NO_3 [Φ_{C_i} of expression (7)] averaged over the 11 h of the simulation as a function of z/h. The flux-gradient relationship of the species is presented in the form of the ratio to the flux-gradient relationship of heat (inert tracer) in order to emphasize the effect of the chemical transformation in the case considered. From the figure we can see that the deviations do not extend above $0.4z/h$ where the flux-gradient relationship of the species is equal to that of heat. The largest deviations are shown by NO_3, which has a flux-gradient relationship that is 20% larger than that of heat. For the other species, the deviations are no larger than a few percent. As demonstrated on other occasions, O_3's flux-gradient relationship is hardly affected because this species is more abundant than the others. Up to $0.2z/h$ the flux-gradient relationship of NO_3 is larger than that of heat and then it becomes smaller. A possible reason for this is again the presence of NO in the first 10% of the NBL. Since the reaction of NO and NO_3 (R3) is very fast (Galmarini et al. 1995), the chemical term in the flux equation of NO_3 is large and affects the flux of this species. The effect decreases rapidly when NO is not present.

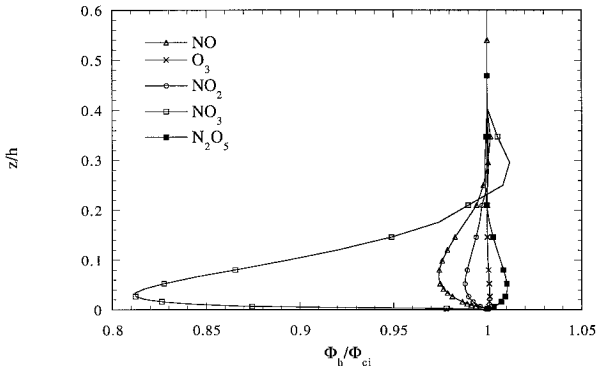

FIG. 5. Flux-gradient relationships of NO, O_3, NO_2, NO_3, and N_2O_5 as a function of z/h. The flux-gradient relationships are normalized with the flux-gradient relationship of heat.

By means of the second-order closure model we have calculated the concentration covariances for the chemical system (R1)–(R6), which, according to expression (5), affect the chemical transformation. From the reactions (R1), (R2), (R3), (R4) the concentration covariances of interest are

$$\overline{\text{no o}_3};\ \overline{\text{no}_2\ \text{o}_3};\ \overline{\text{no no}_3};\ \overline{\text{no}_2\ \text{no}_3}. \tag{8}$$

These are obtained after Reynolds-averaging the mean concentration products. When each of the covariances in expression (8) is divided by the product of the respective mean concentrations we obtain the so-called intensity of segregation (Danckwerts 1952), which defines the state of mixing of the reactants within the turbulent flow. The only calculated intensity of segre-

TABLE 3. The time-averaged turbulent fluxes (ppb ms^{-1}) of the six species at the NBL top.

$\overline{w\ \text{no}_h}$	$\overline{w\ \text{o}_{3h}}$	$\overline{w\ \text{no}_{2h}}$	$\overline{w\ \text{no}_{3h}}$	$\overline{w\ \text{n}_2\text{o}_{5h}}$	$\overline{w\ \text{hno}_{3h}}$
0	-7.97×10^{-4}	2.00×10^{-5}	-7.91×10^{-7}	-5.99×10^{-6}	-8.27×10^{-4}

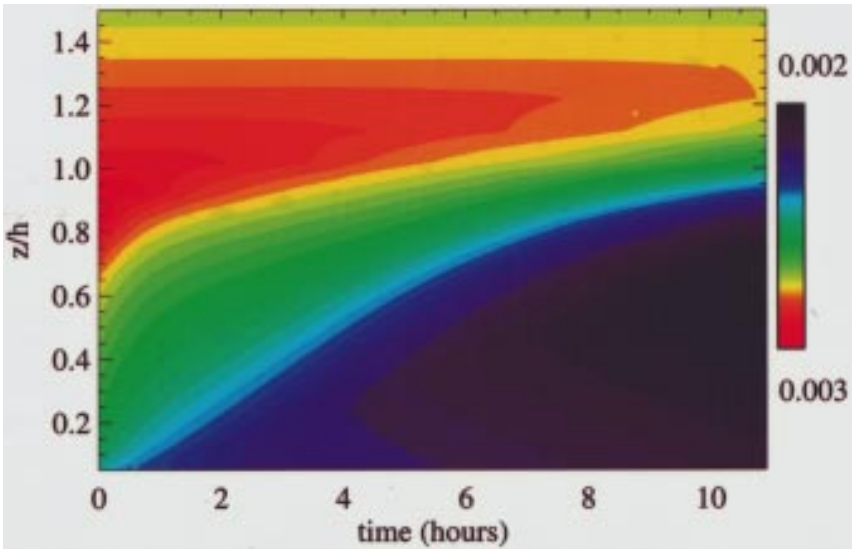

FIG. 6. Space and time evolution of the reaction rate k_5. The color palette indicates the minimum and maximum values (s^{-1}).

gation worth noticing is that between NO and NO_3. It is different from zero throughout the boundary layer and shows a maximum negative value of 4% of the mean concentration. The other concentration covariances listed in (8) hardly exceed 1% during the entire simulated period. The negative value of the covariance between NO and NO_3 has the effect of reducing the efficiency of the chemical reaction [see the chemical term of expression (5)] with a consequent reduction in the production of NO_2. The orders of magnitude determined are in agreement with those found by Galmarini et al. (1997b) for the surface layer. In general, it can be concluded that in a one-dimensional analysis inhomogeneous mixing of the species considered has negligible effects on the mean chemistry of the NBL.

e. Sensitivity analysis

The nocturnal chemical scheme (R1)–(R6) was studied under initial conditions other than those presented in the previous sections. A sensitivity analysis was performed on both the initial conditions of chemical species and the strength of the stable stratification of the NBL. Three other cases were analyzed, namely,

1) same initial conditions of section 2a for the chemical species but $h/L = 2$;
2) surface NO concentration of 4 ppb, $NO_2 = 15$ ppb, $O_3 = 50$ ppb, $h/L = 1$; and
3) same concentration as case 2 but $z/h = 2$.

The increased stability was obtained by maintaining the initial and boundary conditions for the dynamic and thermodynamic variables presented in section 2a, the only difference being a wind speed assumed in this case to be equal to 7 m s^{-1}.

The analysis of these three cases shows that the chemical species behave in almost the same way as for the case presented in section 3. Furthermore, it reveals that for cases 2 and 3 (polluted cases), the initial concentration of NO does not affect qualitatively its and O_3's conversion into NO_2, NO_3, N_2O_5, and ultimately HNO_3. The reaction with O_3 rapidly consumes the entire NO present in the layer, recreating conditions analogous to those presented in section 3. The cases with an increased value in the stability parameter value (cases 1 and 3) do not show substantial differences from the case presented in section 3.

f. The effect of temperature variability on the reaction rates during nighttime

As mentioned earlier, the dependence of the reaction rates on temperature is explicitly accounted for in the model simulation. The reaction rate that shows the largest sensitivity to temperature variations is k_5 (R5). In Fig. 6 the time and space variability of k_5 is plotted. As can be seen, the gradual cooling of the boundary layer generates a gradual reduction in the reaction rate, whereas in the reservoir layer the reaction rate remains more or less constant during the entire simulation. The difference between the maximum and the minimum values is as high as 30%. The sensitivity of reaction rate to temperature is a well-established fact but there are still uncertainties concerning the real temperature dependence (Wayne et al. 1991; Ljungström and Hallquist 1996). The other reaction rates of the scheme (R1)–(R6) show a similar variability in time and space but a smaller variation in order of magnitude. This result not only underlines the importance of making an accurate estimate of the reaction rate for the chemical reactions con-

sidered, but it also demonstrates that it is necessary to take the temperature dependence into account with respect to nighttime conditions. Typical cooling rates of the NBL can range from 0.5 to 2 K h^{-1} (Stull 1988). Under strong cooling, the space and time inhomogeneity of the chemical activity can influence the efficiency of the chemical transformation even more strongly.

4. Comparison with a box model

As indicated by the concentration profiles presented in the previous section, during nighttime conditions the species considered show a large vertical inhomogeneity. In this section we calculate the differences between a detailed one-dimensional description of the turbulent transport of chemically reactive species in the NBL and a description based on a simpler approach, namely a box model (zero-dimensional model). The main characteristic of this type of model is that the concentrations of the species are assumed to vary only in time. The model does not incorporate spatial (vertical) variability. The results presented in this section could be extended to large-scale models in which a coarse grid does not allow for an appropriate resolution of the shallow NBL and the vertical inhomogeneities of the concentration of the species. The problem of space averaging in photochemical models has been considered in the past by Vilà-Guerau de Arellano et al. (1993) with specific reference to horizontal averaging and by Pyle and Zavody (1990) in relation to one-dimensional stratospheric models.

The box model considered here determines the time evolution of the species indicated in reactions (R1)–(R6). To compare the one-dimensional model results with those of the box model, we obtained the initial concentrations of the species in the box model by integrating the initial concentrations of the one-dimensional model in the vertical. The initial concentration of the generic species C_i in the box model is thus given by

$$\langle C_i \rangle_{t=0} = \frac{1}{H} \int_0^H C_i(z, 0)\, dz, \tag{9}$$

where C_i $(z,0)$ is the concentration profile of species C_i in the one-dimensional model at time $t = 0$, H is a constant height (298 m) chosen above the height of the NBL, and the brackets represent the vertical average operator. Since the concentrations in the one-dimensional model are assumed to be horizontally homogeneous, expression (9) can also be interpreted as a volume average. The turbulent fluxes of the species obtained from the one-dimensional model at the surface and at H are used to update the concentrations at each time step. This is done in order to reduce to a minimum the differences between the one-dimensional model and the box model and simply to account for the differences produced by space averaging. As mentioned earlier, the reaction rates in the one-dimensional model are assumed to be temperature dependent and consequently space dependent. The reaction rates of the box model are thus obtained as for (9):

$$\langle k_i \rangle(t) = \frac{1}{H} \int_0^H k_i(z, t)\, dz. \tag{10}$$

The reaction rates of the six species are updated during the time simulation according to (10).

In Figures 7a–f, the time evolution of the volume-averaged concentrations of six species of the chemical scheme (R1)–(R6) obtained with the one-dimensional model is compared with the concentrations obtained with the box model described above. From the figure, one can see that although the box model is able to reproduce the trends of the single species it makes an overall underestimation of all the species, the only exception being NO_2, which is clearly overestimated. It is worth mentioning that the small differences found between the box model and the one-dimensional model depend on the fact that the fluxes at the surface and at the bottom of the box model are the same as those produced by the one-dimensional model.

The different results obtained with the box model are due to subgrid-scale terms. Because of expressions (9) and (10), the concentration and reaction rate fluctuations from the one-dimensional model profiles are given by

$$C_i'(z, t) = C_i(z, t) - \langle C_i \rangle_t;\ k_i'(z, t) = k_i(z, t) - \langle k_i \rangle_t, \tag{11}$$

where the subscript t indicates time dependence.

The volume-averaged concentration of the one-dimensional model and the results of the box model can be compared by making use of (9), (10), and (11). In fact, if one considers the species C_j reacting with C_m at reaction rate k_{jm} and producing C_i, the following expression can be derived:

$$\begin{aligned} \langle k_{mj} C_m C_j \rangle_t = {} & \underbrace{\langle k_{mj} \rangle_t \langle C_m \rangle_t \langle C_j \rangle_t}_{\text{I}} \\ & + \underbrace{\langle k_{mj} \rangle_t \langle C'_m C'_j \rangle_t}_{\text{II}} + \underbrace{\langle C_j \rangle_t \langle k'_{mj} C'_j \rangle_t}_{\text{III}} \\ & + \underbrace{\langle C_j \rangle_t \langle k'_{mj} C'_j \rangle_t}_{\text{IV}} + \underbrace{\langle k'_{mj} C'_m C'_j \rangle_t}_{\text{V}}, \end{aligned} \tag{12}$$

where the left-hand side is the volume average of C_i produced by the one-dimensional model and the right-hand side is the volume-averaged value of the box model. Term II on the right-hand side is the resolved rate of production of C_i in the box model, whereas the other four terms can be seen as subgrid-scale terms of the box model. Any difference between the results of a one-dimensional model and those of a box model is due to the fact that terms III, IV, V, and VI are not accounted for in the box model. These terms are concentration covariances (III), covariances of concentration fluctuations and reaction rate fluctuation (IV, V), and third-order covariances of concentration fluctuations and reaction rate fluctuations (VI).

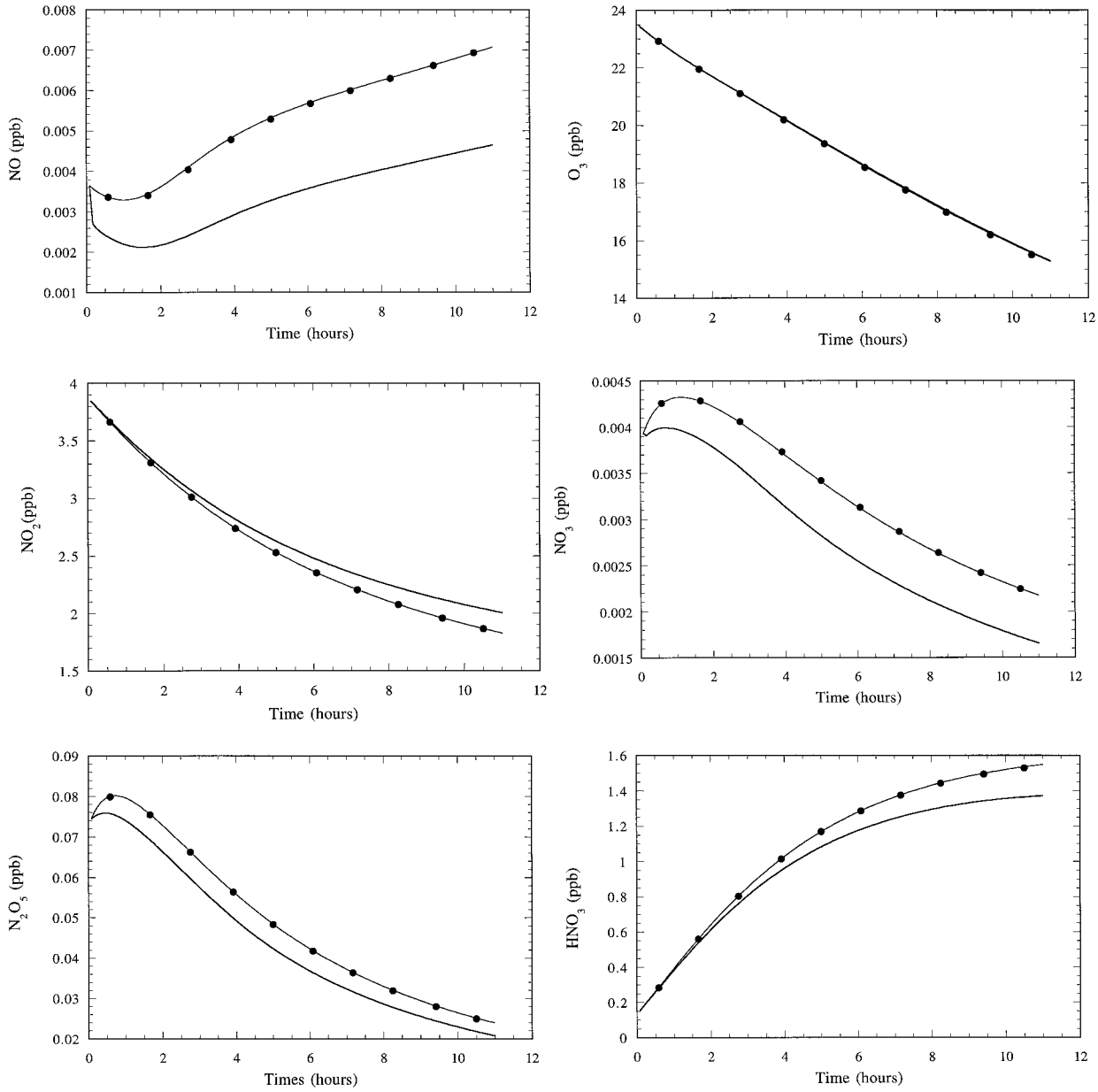

FIG. 7. (a)–(f) Time evolution of the six chemical species of the scheme (R1)–(R6) obtained with the one-dimensional model (integrated in the vertical direction) (thin line), the box model (thick line), and the box model to which the subgrid-scale terms of expression (12) have been added (dots): (a) NO, (b) O_3, (c) NO_2, (d) NO_3, (e) N_2O_5, and (f) HNO_3.

Using the results of the one-dimensional model and of the box model described above we can calculate the budget of the terms expressed in (12) for the chemical scheme (R1)–(R6) in order to determine the role of each subgrid-scale term III, IV, V, and VI in producing the differences between the two modeling approaches. In Fig. 8, the budget of the terms expressed in (12) is presented as a function of time for reactions (R1) and (R3) (Figs. 8a and 8b, respectively). Each term appearing in the figures has been normalized with the resolved-chemistry term of the box model (term II) for the relative chemical reaction. From the figure we see that for reactions (R1) and (R3), in spite of the fact that all terms are different from zero, the most important subgrid term of (8) is term III. Term III normalized with term II represents the state of mixing of the species within the box model. By analogy with the results presented in subsection 3d, term III represents the box model intensity of segregation. For all the other reactions, the budget of the terms of expression (12) gives terms that contribute less than 1% to the subgrid part, so they have not been shown. The terms involving the covari-

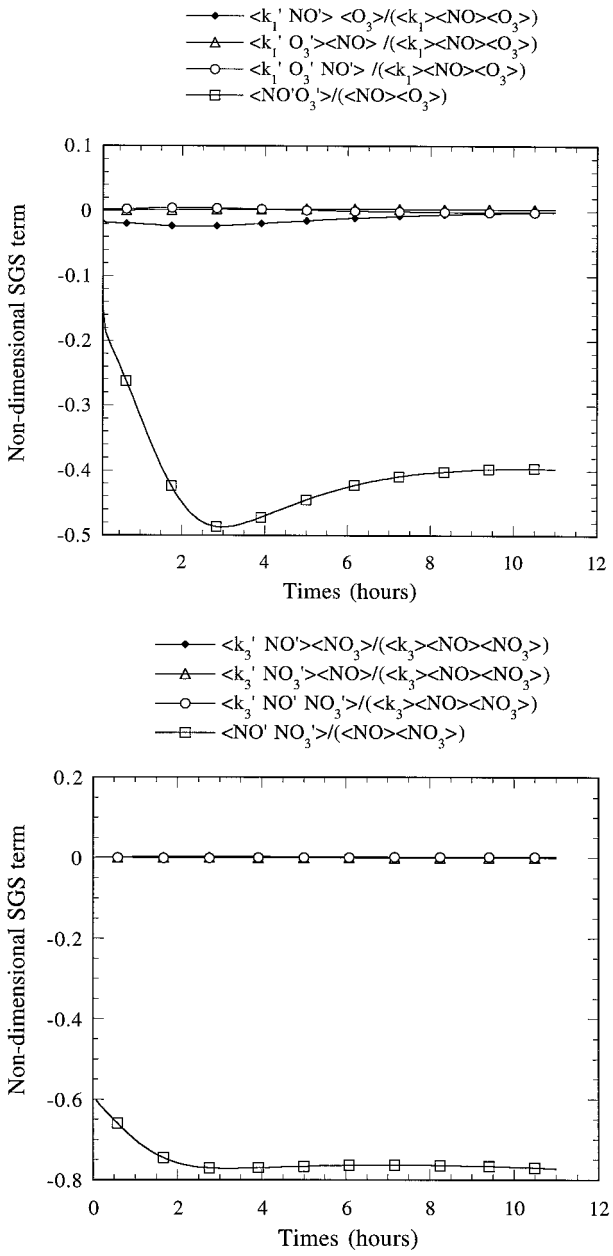

FIG. 8. (a) and (b): Time evolution of the terms III, IV, V, and VI of Eq. (12) calculated for reaction (R1) and (R3), respectively. Each term has been normalized with term II of the same expression.

ance between the concentration fluctuation and the reaction rate concentration are generally very small for all the chemical reactions (one or two orders of magnitude smaller).

From the results of Fig. 8, we can determine the presence of two dominant subgrid-scale terms in the box model (in nondimensional form):

$$\frac{\langle \mathrm{no}'\mathrm{o}_3'\rangle}{\langle \mathrm{NO}\rangle\langle \mathrm{O}_3\rangle} \quad \text{and} \quad \frac{\langle \mathrm{no}'\mathrm{no}_3'\rangle}{\langle \mathrm{NO}\rangle\langle \mathrm{NO}_3\rangle}, \tag{13}$$

obtained from reactions (R1) (Fig. 8a) and (R3) (Fig. 8b), respectively. As one can see, they account for almost 50% and 80% of the resolved part of the relative chemical reactions. The reason for these large values is that the extension of the concentration of NO is limited in the vertical direction due to the chemical depletion caused by the presence of O_3 and NO_3 throughout the NBL. Terms (13) are both negative and after approximately 2 h they tend to asymptotic values. This means that, since terms (13) multiplied by $\langle k_1\rangle\langle \mathrm{NO}\rangle\langle \mathrm{O}_3\rangle$ and $\langle k_3\rangle\langle \mathrm{NO}\rangle\langle \mathrm{NO}_3\rangle$ are equivalent to a reduced production of NO_2 (they are both negative) and consequently to a reduced consumption of NO, O_3, and NO_3, a box model that does not take them into account would constantly overestimate the concentration of NO_2 and underestimate the concentrations of NO, O_3, and NO_3 when compared with one-dimensional model results. This conclusion is confirmed by the results shown in Figs. 7a–d. Expression (13) can be seen as an effective variation of the reaction rate of (R1) and (R3). Using expression (12) and neglecting terms IV, V, and VI, the time evolution of NO, for example, can be written as

$$\frac{\partial\langle \mathrm{NO}\rangle}{\partial t} = -k_{1\ \mathrm{eff}}\langle \mathrm{NO}\rangle\langle \mathrm{O}_3\rangle - k_{3\ \mathrm{eff}}\langle \mathrm{NO}\rangle\langle \mathrm{NO}_3\rangle,$$

where the reaction rates are defined as

$$k_{1\ \mathrm{eff}} = k_1\left(1 + \frac{\langle \mathrm{no}'\mathrm{o}_3'\rangle}{\langle \mathrm{NO}\rangle\langle \mathrm{O}_3\rangle}\right);$$

$$k_{3\ \mathrm{eff}} = k_3\left(1 + \frac{\langle \mathrm{no}'\mathrm{no}_3'\rangle}{\langle \mathrm{NO}\rangle\langle \mathrm{NO}_3\rangle}\right). \tag{14}$$

According to the values obtained for expressions (13), one can see that the effect of the heterogeneous distribution of the species with height in the one-dimensional model can be regarded as an effective variation of the reaction rate in the box model. This variation produces the different behavior obtained with the box model shown in Fig. 7, and it is independent of the order of magnitude of the concentration of the species or the value of its reaction rate.

5. Conclusions

The nocturnal chemistry of nitrogen oxides has been studied by means of a one-dimensional turbulence-closure model. The model describes the formation and the time evolution of a stably stratified NBL and the evolution of six typical nighttime chemical species, namely NO, O_3, NO_2, NO_3, N_2O_5, and HNO_3. This set of chemical species has been chosen because it is representative for the nighttime chemistry of nitrogen oxides and because it contains species (NO_3 and N_2O_5) that act as reservoirs for the daytime triad NO–NO_2–O_3 and species (HNO_3) by means of which the triad is removed from the atmosphere. The turbulent fluxes of the chemical species have been determined by means of a second-order closure model. This approach allows one to take explicitly into account the chemical

reaction as a production/depletion term for the flux of the species. The initial and boundary conditions for the chemical species have been chosen on the basis of typical rural concentration values. As far as the chemical species are concerned, the results reveal that chemistry in the stable boundary layer can be decoupled from that of the so-called reservoir layer. This result is supported by the experimental evidence. The species emitted at the surface (NO) can hardly be transported above 10% of the boundary layer depth due to the reduced turbulent activity and to the fast chemical reaction with O_3. The limited range of transport of NO influences the overall chemical scheme. The analysis of the turbulent fluxes reveals that local flux maxima arise due to the local chemical activity. The NO_2 flux in particular changes sign due to local production of the species. The influence of chemical transformation on the flux of the species has been investigated. The results show that the flux that is most sensitive to chemical transformation is that of NO_3. It can be as much as 20% larger than the flux of an inert tracer. The effect of chemical reaction on the flux of the species reduces with height and does not extend beyond 50% of the boundary layer depth. The model explicitly accounts for the temperature dependence of the reaction rates of the scheme considered. The case considered reveals that in the case of an NBL, where temperature can vary considerably in space and time, this dependence may cause large variations in the chemistry activity in the boundary layer and in the reservoir layer. The difference between the maximum and the minimum rate of the thermal dissociation of N_2O_5 can be as much as 30%.

The detailed one-dimensional description of the nocturnal chemistry has been compared with a simpler zero-dimensional approach. The aim of the study was to determine the reasons for the differences between the two modeling approaches. These differences arise from the presence of large vertical inhomogeneity in the distribution of the species. Budgets of the subgrid-scale terms of a box model have been presented. The results show that the largest contribution to the differences between the two approaches stems from the covariance between concentration fluctuations in space. Given the distribution of the nighttime nitrogen oxides during the formation and the evolution of a stable boundary layer, the concentration covariances between NO and O_3 and those between NO and NO_3 can affect the overall determination of the concentration of NO and NO_3 when a box model is used.

Acknowledgments. The authors are grateful to Dr. U. Neu for kindly providing the Air Pollution and Meteorology (POLLUMET) experiment data and to Dr. Maarten Krol and Prof. Jos Lelieveld for making useful suggestions and comments.

APPENDIX

In this appendix the reaction rates of the chemical system (R1)–(R6) are per cubic centimeter per mole per second. The expressions have been taken from Atkinson et al. (1992):

$$k_1 = 1.8e^{-12}e^{-1370/T}$$

$$k_2 = 1.2e^{-13}e^{-2450/T}$$

$$k_3 = 1.8e^{-11}e^{110/T}$$

$$k_4 = \frac{k_4' k_4''}{k_4' k_4''} F,$$

where

$$k_4' = 2.7\left(\frac{T}{300}\right)^{3/4} e^{-30} \quad k_4'' = 2\left(\frac{T}{300}\right)^{1/5} e^{-12}$$

$$k_5 = \frac{k_5' k_5''}{k_5' k_5''} F,$$

where

$$k_5' = 2.2\left(\frac{T}{300}\right)^{-4.4} e^{-3}e^{-11080/T}$$

$$k_5'' = 9.7\left(\frac{T}{300}\right)^{1/10} e^{-5}e^{-11080/T}$$

$$k_6 = 2e^{-21}.$$

The term F appearing in k_4 and k_5 is given by

$$F = e^{-T/250} + e^{-1050/T}.$$

REFERENCES

Atkinson, R., D. L. Baulch, R. A. Cox, R. F. Hampson Jr., J. A. Kerr, and J. Troe, 1992: Evaluated kinetic and photochemical data for atmospheric chemistry. Supplement IV. IUPAC subcommittee on gas kinetic data evaluation for atmospheric chemistry. *J. Phys. Chem. Ref. Data,* **21**(6), 1125–1568.

Chatfield, R. B., and A. C. Delany, 1990: Convection links biomass burning to increase tropical ozone: However, models will tend to overpredict O3. *J. Geophys. Res.,* **95**(D11), 18 473–18 488.

Danckwerts, P. V., 1952: The definition and measurement of some characteristic mixtures. *Appl. Sci. Res.,* **A3,** 279–296.

Davidson, J. A., C. A. Cantrell, R. E. Shetter, A. H. Mc Daniel, and J. G. Calvert, 1990: The NO_3 radical composition and NO_3 scavenging in the troposphere. *J. Geophys. Res.,* **95,** 13 963–13 969.

Dentener, F. J., and P. J. Crutzen, 1993: Reaction of N_2O_5 on tropospheric aerosol: Impact on the global distributions of NO_x, O_3, and OH. *J. Geophys. Res.,* **98**(D4), 7149–7163.

Donaldson, C. duP., and G. R. Hilst, 1972: The effect of inhomogeneous mixing on atmospheric photochemical reactions. *Environ. Sci. Technol.,* **6,** 812–816.

Duynkerke, P. G., 1991: Radiation fog: A comparison of model simulation with detailed observations. *Mon. Wea. Rev.,* **119,** 324–341.

England, C., and W. H. Cocoran, 1974: Kinetics and mechanisms of the gas-phase reaction of water vapor and nitrogen dioxide. *Ind. Eng. Chem. Fundam.,* **13,** 373–384.

Estournel, C., and D. Guedalia, 1985: Influence of geostrophic wind on atmospheric nocturnal cooling. *J. Atmos. Sci.,* **42,** 2695–2698.

Finlayson-Pitts, B. J., and J. N. Pitts, 1986: *Atmospheric Chemistry. Fundamentals and Experimental Technique.* John Wiley & Sons, 850 pp.

Fitzjarrald, D. R., and D. Lenschow, 1983: Mean concentration and flux profile for chemically reactive species in the atmospheric surface layer. *Atmos. Environ.,* **17**(12), 2505–2512.

Galmarini, S., J. Vilà-Guerau de Arellano, and P. G. Duynkerke, 1995: Surface layer scaling applied to chemically reactive species under unstable and stable conditions. Preprints, *11th Symp. on Boundary Layers and Turbulence,* Charlotte, NC, Amer. Meteor. Soc., 568–571.

——, C. Beets, and P. G. Duynkerke, 1997a: Stable nocturnal boundary layer: A comparison of one-dimensional and LES models. *Bound.-Layer Meteor.,* in press.

——, J. Vilà-Guerau de Arellano, and P. G. Duynkerke, 1997b: Scaling the turbulent transport of chemically reactive species in a neutral and stratified surface-layer. *Quart. J. Roy. Meteor. Soc.,* **123,** 223–242.

Gao, W., and M. Wesely, 1994: Numerical modeling of the turbulent fluxes of chemically reactive trace gases in the atmospheric boundary layer. *J. Appl. Meteor.,* **33,** 835–847.

Harrison, R. M., C. D. Holman, H. A. McCartney, and J. F. R. McIlveen, 1978: Nocturnal depletion of photochemical ozone at a rural site. *Atmos. Environ.,* **12,** 2021–2026.

Johnston, H. S., C. A. Cantrell, and J. G. Calvert, 1986: Unimolecular decomposition of NO_3 to form NO and O_2 and a review of N_2O_5/NO_3 kinetics. *J. Geophys. Res.,* **91,** 5159–5172.

LeBel, P. J., B. J. Huebert, H. I. Schiff, S. A. Vay, S. E. VanBramer, and D. R. Hastie, 1990: Measurements of tropospheric nitric acid over western United States and Northeastern Pacific Ocean. *J. Geophys. Res.,* **95**(D7), 10 199–10 204.

Ljungström, E., and M. Halquist, 1996: Nitrate radical formation rates in Scandinavia. *Atmos. Environ.,* **30**(16), 2925–2932.

Mahrt, L., and R. C. Heald, 1979: Comments on ''Determining the height of the nocturnal boundary layer.'' *J. Appl. Meteor.,* **18,** 383.

Mentel, F., and A. Wahner, 1997: A large reaction chamber for nighttime atmospheric chemistry: Design and characteristics of the reaction chamber. *Atmos. Environ.,* in press.

Mihelcic, D., D. Klemp, P. Musgen, H. W. Patz, and A. Volz-Thomas, 1993: Simultaneous measurements of peroxy and nitrate radicals at Schauinsland. *J. Atmos. Chem.,* **16,** 313–335.

Mozurkewich, M., and J. C. Calvert, 1988: Reaction probability of N_2O_5 on aqueous aerosols. *J. Geophys. Res.,* **93,** 15 889–15 896.

Neu, U., T. Kunzle, and H. Wanner, 1994: On the relation between ozone storage in the residual layer and daily variation in the near-surface ozone concentration—A case study. *Bound.-Layer Meteor.,* **69,** 221–247.

Nieuwstadt, F. T. M., 1984a: The turbulent structure of the stable, nocturnal boundary layer. *J. Atmos. Sci.,* **41,** 2202–2216.

Pitts, J. N., Jr., H. M. Biermann, R. Atkinson, and A. M. Winer, 1984: Atmospheric implications of simultaneous nighttime measurements of NO_3 radicals and HONO. *Geophys. Res. Lett.,* **11,** 557–560.

Platt, U., D. Perner, A. M. Winer, G. W. Harris, and J. N. Pitts Jr., 1980: Detection of NO_3 in the polluted troposphere by differential optical absorption. *Geophys. Res. Lett.,* **7,** 89–92.

——, ——, J. Schröder, C. Kessler, and A. Toennissen, 1981: The diurnal variation of NO_3. *J. Geophys. Res.,* **86**(C12), 11 965–11 970.

——, A. M. Winer, and H. M. Biermann, 1984: Measurements of nitrate radical concentrations in continental air. *Environ. Sci. Technol.,* **18,** 365–360.

Pyle, J., and A. M. Zadovy, 1990: Modelling problems associated with space averaging. *Quart. J. Roy. Meteor. Soc.,* **116,** 753–766.

Rao, K. S., and H. F. Snodgrass, 1979: Some parameterizations of the nocturnal boundary layer. *Bound.-Layer Meteor.,* **17,** 15–28.

Russell, A. G., G. R. Cass, and J. H. Seinfeld, 1986: On some aspects of nighttime atmospheric chemistry. *Environ. Sci. Technol.,* **20,** 73–78.

Schuman, U., 1989: Large-eddy simulation of turbulent diffusion with chemical reactions in the convective boundary layer. *Atmos. Environ.,* **23,** 1713–1727.

Seinfeld, J. H., 1986: *Atmospheric Chemistry and Physics of Air Pollution.* John Wiley and Sons, 615 pp.

Slemr, F., and W. Seiler, 1984: Field measurement of NO and NO_2 emissions from fertilized and unfertilized soils. *J. Atmos. Chem.,* **2,** 1–24.

Solomon, S., H. L. Miller, J. P. Smith, R. W. Sanders, G. H. Mount, A. L. Schmeltekopf, and J. F. Noxon, 1989: Atmospheric NO_3. 1. Measurement technique and annual cycle at 40° N. *J. Geophys. Res.,* **94**(D8), 11 041–11 048.

Sorbjan, Z., 1986a: On similarity in the atmospheric boundary layer. *Bound.-Layer Meteor.,* **34,** 377–397.

Stull, R. B., 1988: *An Introduction to Boundary Layer Meteorology.* Kluwer Academic Press, 665 pp.

Sykes, R. I., S. F. Parker, D. S. Henn, and W. S. Lewellen, 1994: Turbulent mixing with chemical reaction in the planetary boundary layer. *J. Appl. Meteor.,* **33,** 825–834.

Venkatram, A., 1993: The parameterization of the vertical dispersion of a scalar in the atmospheric boundary layer. *Atmos. Environ.,* **27A**(13), 1963–1966.

Vilà-Guerau de Arellano, J., P. G. Duynkerke, P. J. Jonker, and P. J. H. Builtjes, 1993: An observational study of time and space averaging in photochemical models. *Atmos. Environ.,* **27A,** 353–362.

——, ——, and K. Zeller, 1995: Atmospheric surface layer similarity theory applied to chemically reactive species. *J. Geophys. Res.,* **100**(D1), 1397–1408.

Wanner, H., T. Kunzle, U. Neu, B. Ihly, G. Baumbach, and B. Steisslinger, 1993: On the dynamics of photochemical smog over Swiss Midland—Results of the first POLLUMET Field Experiment. *Meteor. Atmos. Phys.,* **51,** 117–138.

Warnek, P., 1988: *Chemistry of the Natural Atmosphere.* Vol. 41, *International Geophysics Theory,* Academic Press Inc., 454 pp.

Wayne, R. P., and Coauthors, 1991: The nitrate radical: Physics, chemistry and the atmosphere. *Atmos. Environ.,* **25A,** 1–203.

Webb, E. K., G. I. Pearman, and R. Leuning, 1980: Correction of flux measurements for density effects due to heat and water vapour transfer. *Quart. J. Roy. Meteor. Soc.,* **106,** 48–75.

Wesely, M. L., D. L. Sisterson, R. L. Hart, D. L. Drapcho, and I. Y. Lee, 1989: Observations of nitric oxide fluxes over grass. *J. Atmos. Chem.,* **9,** 447–463.